SSRG International Journal of Electrical and Electronics Engineering
ISSN: 2348-8379/ https://doi.org/10.14445/23488379/IJEEE-V11I11P103

Volume 11 Issue 11, 23-29, November 2024

Original Article

An Approach to Transcutaneous Inductive Power and Data Link for Implantable Biomedical Microsystems

Kadiyam Venkata Sai Subramanyeswara Rao[1], Guntu Raja Rao[2], Kanchapogu Vaisakh[3]

[1,3]*Department of Electrical Engineering, Andhra University, Andhra Pradesh, India.*
[2]*Department of Electrical Engineering, Anil Neerukonda Institute of Technology and Sciences, Andhra Pradesh, India.*

[1]*Corresponding Author : subra.rao99@gmail.com*

Received: 03 September 2024 Revised: 03 October 2024 Accepted: 02 November 2024 Published: 30 November 2024

Abstract - *This paper proposes a practical approach to wireless power and data communication systems for biomedical implants using an inductive power and data transfer link. The system comprises a class E power amplifier/transmitter, an Amplitude-Shift Keying (ASK) modulator, an Inductive Power and Data Link (IPDL) and an ASK demodulator. The modulation circuit comprises a capacitor and a MOSFET to switch the load of the Class-E transmitter between two states, satisfying both zero-voltage switching and derivative switching conditions, leading to higher DC to AC power transfer efficiency. This situation develops ASK data modulation in the class E transmitter. The developed IPDL contains an external class E transmitter part placed external to the human body to transfer wireless power and data to the internal receiver part (implanted device) for exciting and monitoring relevant nerves of damaged tissue. For the safety condition of the tissue, the IPDL system is operated at a selected lower carrier frequency of 4MHz, and the ASK modulator is envisioned to operate with a modulation index of 43% and a modulation rate of 4.3% with a data rate as 172Kbps. A practical IPDL system is presented with results of real-time simulation using TINA ver. 8 and MULTISIM ver12.0 software.*

Keywords - *Wireless power transfer, Data transmission, Inductive link, Class-E power transmitter, Amplitude Shift Keying, Medical implant.*

1. Introduction

The electronic prosthesis devices, namely deep brain stimulator, pacemaker, bionic eye (retinal implants), bionic ear (cochlear implants), and stimulator implants are biomedical devices - Implantable Medical Devices (IMDs) which mimic the behavior of damaged sensors of the human body. The main role of these micro-system stimulators is to generate electrical signals that excite the biological nerves/muscles to provide near-equivalent sensing [1]. The IMDs are powered using batteries that have limited endurance and chemical side effects. Several investigators chose various innovative schemes to power up and observe IMDs [2]. IMDS is generally powered through a transcutaneous path through an IPDL system comprising two parts: the external part and the interior unit. The exterior unit is for transferring power/data induced to the interior component, i.e., IMD placed within the body.

The IPDL between the external RF transmitter and internal receiver is mostly a weak link that definitely needs an efficient modulator and efficient RF Power amplifier [3]. Out of three modulators such as ASK, 'Frequency Shift Key (FSK)', and Phase Shift Key (PSK)', the ASK modulator is preferred for IMDs because of its low power consumption, less complexity, and lower cost, unlike complex multitone PSK modulation used by authors P. Dhull, et al. in [4]. An improved ASK modulator with a modulation index of 43% is shown with 86 KHz frequency and an improved class-E power amplifier, which has been working at carrier 4MHz frequency to eliminate the tissue heating based on the ISM (Industrial, Scientific, and Medical) band [5] for the external transmitter part whereas authors Mohammad Haerinia and Reem Shadid in [13] enumerated use of higher carrier frequencies for driving class-E amplifier that leads to tissue heating problem. The IPDL is designed for an assumed implanted electronic device load resistor as 100-1000Ω with static coupling coefficient k = 0.612. The IPDL is tested practically, and results are shown. The real-time simulation is carried out by using the electronic workbench version MULISIM 12. The second section deals with the overview of IPDL system architecture. The circuit details of ASK modulation are addressed in section three. Section four discussed Class-E RF power amplifier with its component values. Theoretical and practical IPDL characteristics with varied coupling coefficients are given in section five. Experimental data from practical IPDL circuit and IPDL simulated circuit is provided in section six, followed by concluding remarks in the 7th section.

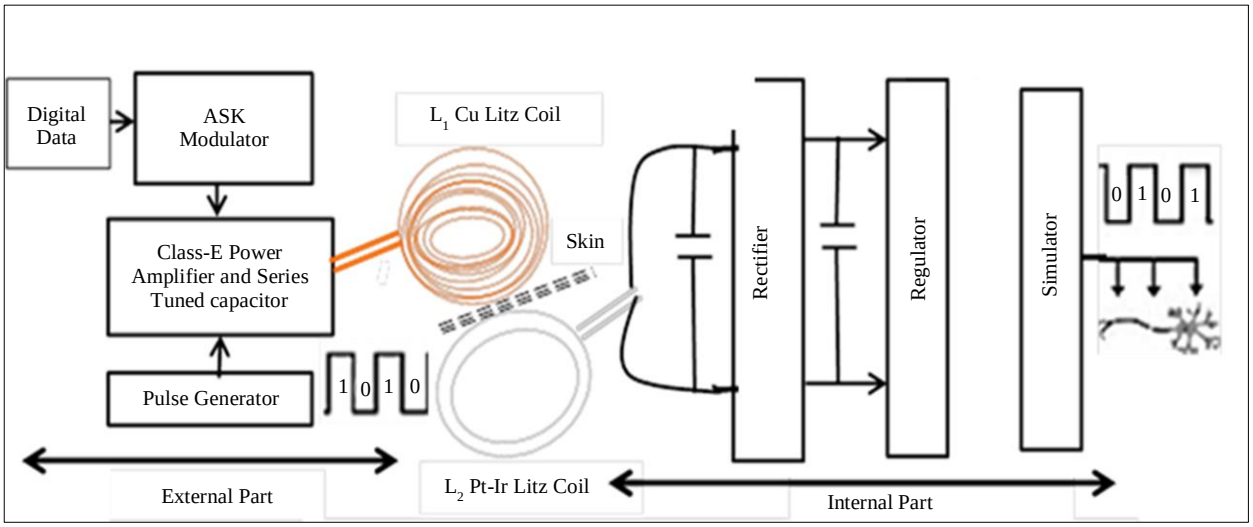

Fig. 1 Block-level view of inductive power/data transmission

2. IPDL System Overview

The IPDL functioning block diagram of the IPDL system for conducting power along with the data transfer digitally in IMDs is presented in Figure 1. An IPDL system includes an external part placed external to the human body. The exterior unit comprises a power supply, ASK modulator with binary data input, Class-E Power Amplifier (P/A) with 4MHz pulse generator, and transmit Cu Litz coil. The interior unit comprises a receive Pt-Ir Litz coil, a rectifier to get power and data, a voltage regulator to get constant DC-voltage to IMD, and remote electronics/Stimulator including an ASK-demodulator to get the stimulating signal to the tissue. The coupled inductive links comprise two RLC circuits tuned at 4MHz resonant frequency. The RLC circuit at the transmitter side is tuned at serial resonant with a lesser impedance load, and the receiver side RLC circuit has been synchronized for a parallel resonance cap. C_2 [6, 12, 14]. A schematic of a class-E RF power amplifier circuit, which has been designed and depicted in Figure 2, couples the external part to the internal part for the transfer of 'power and data' together efficiently. For an inductive/magnetic coupling system, the compensation capacitors can be connected in two different ways: parallel to both sides of the inductors and in series. These connections have produced four different topologies: Series-Series (SS), Parallel-Series (PS), Series-Parallel (SP), and Parallel-Parallel (PP). Table 1 lists the performance details for each topology. In the present paper, SP topology is used for higher efficiency of inductive links.

Table 1. Compensation capacitor topologies

Topology	Acts as Source	Independent of Changes	Impedance@ Resonance	Efficiency
SS	Current	C_s	Lower	Very Higher
SP	Voltage	C_s	Lower	Higher
PS	Voltage	C_s	Higher	Medium
PP	Current	C_p	Higher	Higher

3. ASK Modulator Design

The ASK RF transmission logic circuit depicted in Figure 2 is a Class-E power amplifier having a MOSFET transistor driven by a fixed frequency of resonance frequency ω_0 with Lp(9μH), Cp(141pF) circuit. Data is transmitted by ASK modulation, developed by changing the power supply used in 'ASK' modulation, as in other schemes, which is preferred by altering the amplifier frequency response. A scope existed for optimizing energy transmission with dissipative components not used in modulation [7, 13, 25]. Based on the data driving the MOSFET Q_{mod}, the resonant tank's transfer function will be modified. Then, 2 separate levels would be transmitted for unipolar NRZ data as ''0'' and ''1'' utilizing the same carrier frequency and the power in the ASK transmitter could be controlled via class E amplifier power supply (Vdd) because the ASK circuit or its response of frequency is changed [25, 27].

The proposed RF transmitter gives an advantage in that tuning of IPDL is possible to 1 frequency, and this level could be allocated to a digital logic level "1" [25]. Under no data, the efficiency is higher because the same level is transmitted

all the time. For another logic level, "0", if transmitted, reduced efficiency is possible because of the change in fine-tuning of the amplifier [25]. The intended circuit lessens this impact and makes it possible to achieve greater transmitting power efficiency because additional modulating logic (a transistor that controls power from the amplifier supply or defines the transmitting level) is not required [25].

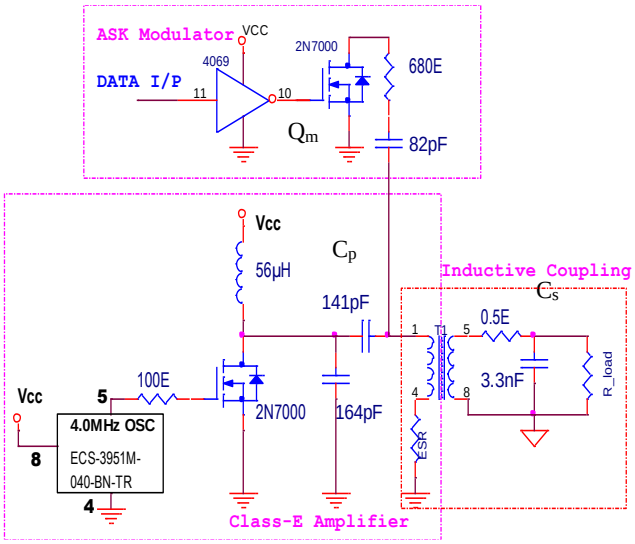

Fig. 2 Schematic of class E Amp/ASK modulator with SP compensation capacitor topology

Amplitude-shift keying modulation is a popular choice for IMDs due to:

1. Simple modulation technique to implement.
2. Low power operation.
3. Ease of demodulation.
4. Compatibility with power transfer.

Transmission speed may be raised by increasing the carrier frequency with suitable design of circuits. The modulating schematic in Figure 2 uses MOS transistor Qm, the resistor, and the capacitor to adjust the MI with a value of 43% and MR with a value of 4.3%. The binary data with a bit rate of 5.8 µs is employed from the pulse generator, as shown in Figure 1.

With values of "1" and "0," the binary data signal for the ASK modulator is shown in Figure 3(a). In Figure 3(b), the ASK modulated signal at the transmitter coil with V_{max}=30V and V_{min}=12V is shown. The formulas in (1 and 2) are used to calculate the MI and MR, where Vmax & Vmin stand for the max and min amplitudes for ASK modulation, respectively.

$$MI = (V_{max}-V_{min})/(V_{max}+V_{min})\%100 \quad (1)$$

$$MR = (\text{Data Rate})/(\text{Operating Frequency}) \times 100\% \quad (2)$$

With Vmax = 4.8V and Vmin = 2.0V, Figure 3(c) displays received ASK modulation at the receiving coil. It is observed that the MI is the same for the transmitter and receiver coils on both sides.

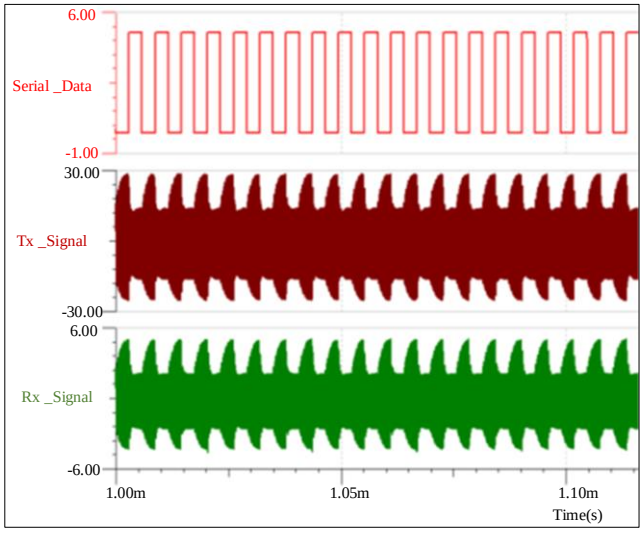

Fig. 3(a) The binary serial data signal, (b) ASK Tx Signal, and (c) ASK Rx signal at the bottom in the above picture have approximately the same modulation index.

4. Class-E Power Amplifier at 4 MHz

Because it eliminates the need for a mixer and has a high theoretical efficiency of 90-95%, Class-E power amplifiers are broadly utilized in biotelemetry and external RF transmitters of IMDs. They also consume less power when used with ASK modulators because they are high-energy transmitters [7]. A parallel capacitor is connected to an NMOS switching transistor to enable zero-voltage switching of non-ideal NMOS transistors.

An RF choke with negligible resistance prevents drops in the Vdd power supply. These components make up the structure of the class-E power amplifier. A specific frequency is chosen to tune an RLC network to achieve a constant current from the supply source. In addition, the RLC network converts the digital input signal into a sinusoidal output signal with no Direct Current (DC) component.

To minimize tissue damage, the class-E power amplifier was designed to operate at a low band frequency of 4MHz [8, 15, 14]. The mathematical model involves a P_{out} of 150mw, f_0 = 10MHz, V_{DD} =3.3V; R_L (load resistor) is 50Ω, and Equation (3) is for calculating the optimum resistance R_{Lopt}. [9, 16]. Equations (4), (5), and (6) are for calculating values of class – E components, as in Figure 4.

$$Pout = \{2/(1+\pi^2/4)\} \times \{V^2_{DD}/R_{Lopt}\} \quad (3)$$

$$Cp = \{1/\omega_0 R_L(1+\pi^2/4)\,(\pi/2)\} = \{1/\omega_0(5.447R_L)\} \quad (4)$$

$$Lp = QR_L/\omega_0 \quad (5)$$

$$Cs = Cp\ \{5.447/Q\}\{1+1.42/(Q - 2.08)\} \quad (6)$$

The Quality factor (Q), which reduces the bandwidth of the IPDL system, should be at maximum for maximum efficiency in order to produce an output that is as close to sinusoidal as possible [10, 17]. The selection of Q needs to be realistic, and it is calculated as 27 according to Equation (7).

$$Q \leq (\omega L)/R \quad (7)$$

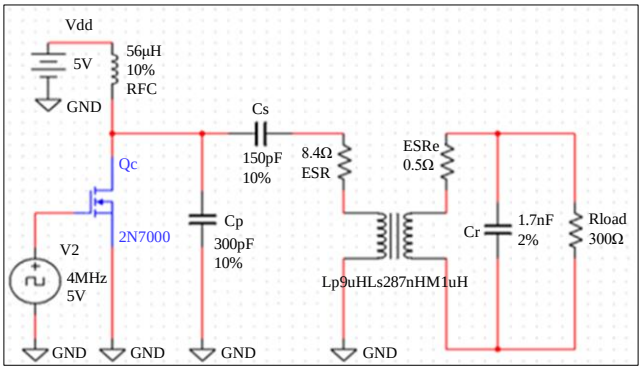

Fig. 4 Schematic of class-E power amplifier with 50% duty cycle of switch Q_c.

Reduce Qc transistor switching losses to make a class-E power amplifier with high efficiency. Qc is activated when its drain voltage reaches zero again. As shown in Figure 5, the drain voltage has been increased from 0 at the point of activation, allowing for a slight decrease without affecting effectiveness.

Fig. 5(a) V_{DS}- drain to source voltage and V_{GS} gate to source voltage pulse waveforms from MULTISIM 12

The drain to source voltage signal V_{DS} of MOSFET Q_c in Figure 5 shows a peak voltage of 14V when its gate drive signal V_{GS} is zero, and the primary resonant tank circuit gets charged. When V_{GS} is +5V pulse, the peak value of V_{DS} of MOSFET Q_c is +0.5V.

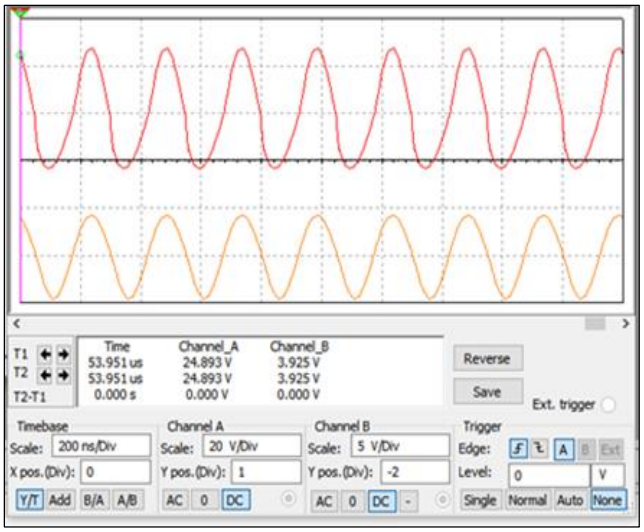

Fig. 5(b) ASK Tx coil and Rx coil voltages output signals

5. Inductive Powering Links

IMDs are generally powered inductively for power as well as data transfer at a short range. As seen in Figure 6 [11, 18, 19], IPDL comprises two resonant RLC circuits.

The first is called the primary part, external part, or in vitro part, and it is situated outside the human body. It is powered by an effective RF class E power amplifier. A portion of the magnetic flux generated by the external part is coupled to the secondary coil, which serves as an antenna, powering the secondary, internal, or vivo part.

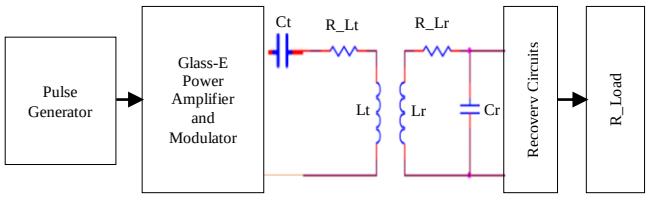

Fig. 6 Block diagram of IPDL

As can be seen in Figure 2, the SP capacitive compensation topology is used to tune the primary and secondary coils at the same resonant frequency in order to increase power transfer efficiency. The coupling link efficiency is directly affected by the variables involved in the inductive coupling link are the coupling factor (also known as the coupling coefficient, denoted as k, which must be between 0 and 1), resonant frequency (f0), mutual inductance (M), primary coil inductance (Lp), secondary coil inductance (Ls), and the coupling factor. The coupling factor K is the primary determinant of the power capacity for implanted devices [12, 20, 21]. The coupling coefficient,

or "k," is clearly reliant on the flux that connects the primary coil inductance, or "mutual inductance," L_t, to the secondary coil inductance, L_r. The ratio of M to the square root of the product of L_p & L_s is how M and k are expressed in Equation (8).

$$k = M/\sqrt{L_p L_s} \quad (8)$$

The resonant capacitor Cp across $Q_c$value can be calculated using the Equation (4). Another resonant capacitor Cr value can be calculated using the Equation (9).

$$Cs = \{R_{load} + \sqrt{R^2_{load} - 4\omega_0^2 L_s^2}\}/\{2\omega_0^2 R_{load} L_s\} \quad (9)$$

R_{load} is assumed to be the IMD's load resistance [13, 22-24] which is usually greater than $2\omega L_s$.

When the primary and secondary coils are tuned to the identical resonant frequency of 4 MHz, the TINA simulation results in Figure 7 show that the IPDL functions as a band pass filter with a center frequency of 4 MHz.

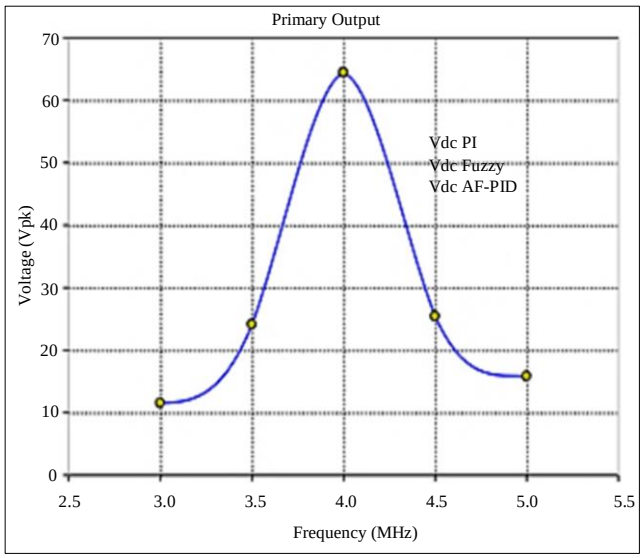

Fig. 7(a) Primary Tx coil voltage Vs Frequency graph

The outcomes of the TINA simulation in Figure 8 depict the correspondence between the constant load resistor at value 250Ω with variable coupling coefficients as K= 0.5, K= 0.6, K= 0.7, K= 0.8, and it is found that maximum voltage gain (prim. Tx Volt./second RxVolt) is observed at K=0.8.

It is concluded from the simulation outcomes in Figures 7, 8, and 9 that the IPDL design is suitable for powering IMDs with R_{load} from 100Ω to300Ω.

Further, it can be pointed out that R_{load} may be treated as a function of the amplitude of secondary R x coil voltage, and larger Rx coil voltage indicates more power consumption.

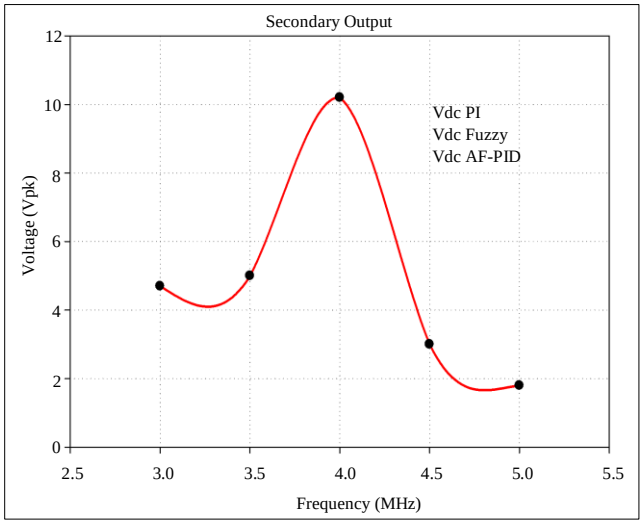

Fig. 7(b) Secondary Rx coil voltage vs Frequency graph

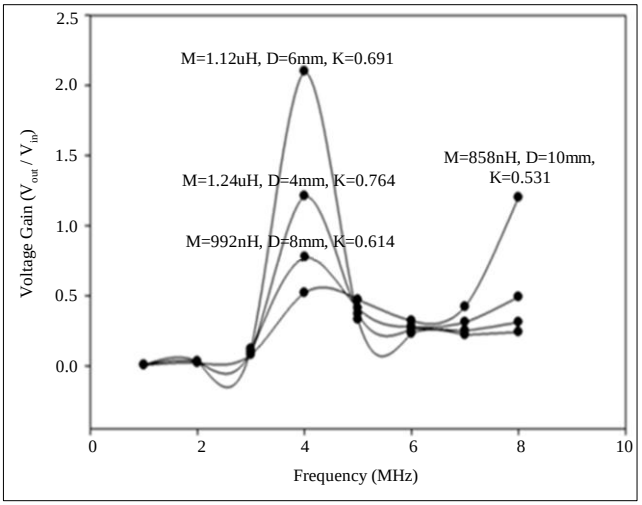

Fig. 8 Voltage gain vs frequency graph with variable K and fixed load resistance R_{load} of 250 Ohms

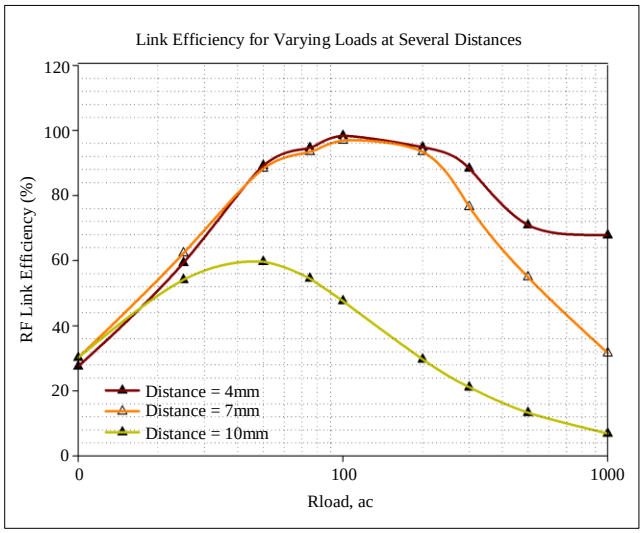

Fig. 9 RF link efficiency vs Variable load graph with variable IPDL distances of 4mm, 7mm, and 10mm

6. Results from MULTISIM 12 Simulation

Simulation software such as TINA 8 and MULTISIM 12 simulate the IPDL system architecture. The results of the TINA simulation, as shown in Figure 3(a), correspond to binary serial data signals with "1" and "0" values that are supplied to the ASK modulator with 100ps rise/fall times with a frequency of 86.2KHz (172Kbps). ASK modulated signal on the transmission coil with Vmax = 30V and Vmin = 12V is depicted in Figure 3(b). ASK modulated signal with a maximum voltage of 4.8V and a minimum voltage of 2V is shown at the receiving coil in Figure 3(c).

The Modulation Index (MI) as well as Modulation Rate (MR) for transmitted as well as received signals are 43% and 4.3% respectively. Figure 5 shows the results of simulating Class-E power amplifier by MULTISIM 12. Figure 5(a) shows two waveforms such as Qc MOSFETS's Gate to Source Voltage (VGS) drive pulses at 86.2KHz driving Qc ON & OFF to generate Qc's Drain to Source Voltage (VDS) pulses for generating sinusoidal output current in primary Tx coil Lp and Figure 5(b) shows the primary Tx coil output signal of the power amplifier with the best efficiency ηopt of 81% based on optimal k, quality factors Qp and Qs of primary and secondary coil [26] as given in (10).

$$\eta opt = \frac{k^2 Q_p Q_s}{[\,1+\sqrt{1+k^2 Q_p Q_s}\,]^2} \tag{10}$$

Furthermore, a good sinusoidal wave is generated by the class-E power amplifier for IPDL, improving overall IPDL efficiency.

7. Conclusion

The authors presented a design of an external module of a practical transcutaneous efficient IPDL system for IMDs for the human body to transmit with a carrier of 4MHz and ASK modulation of the power with data to implanted devices. Three parts of the external primary module were developed and simulated with OrCAD Pspice16.2 software tools and TINA 8 and MULTISIM-12. It is observed that IPDL can transfer an improved power to IMDs with a data rate of 0.2 Mbit/s and MI 43%. The IPDL can be used in IMDs with a 100 to 1000 ohms load range.

This paper presented a Simultaneous Wireless Power and Data Transmission System (SWPDTS) on one pair of coils with higher power efficiency delivery and forward data transmission. An extensive simulation of the proposed SWPDTS is performed to evaluate the safety and reliability of the SWPDTS, attaining around 10,000 data bits. Future work may include bidirectional data transmission between the external/primary system and the internal/secondary system for the IPDL. In conclusion, the proposed SWPDTS provides high power and data transmission performance and has the potential for IMD applications requiring higher data rates, lesser power drain, and higher power transfer efficiency.

References

[1] Mohamed Ghorbel et al., "An Advanced Low Power and Versatile CMOS Current Driver for Multi-Electrode Cochlear Implant Microstimulator," *Journal of Low Electronics*," vol. 2, no. 3, pp. 442-455, 2006. [CrossRef] [Google Scholar] [Publisher Link]

[2] Maysam Ghovanloo, and Suresh Atluri, "A Wideband Power-Efficient Inductive Wireless Link for Implantable Microelectronic Devices Using MultIPDLe Carriers," *2006 IEEE International Symposium on Circuits and Systems (ISCAS)*, Kos, Greece, 2006. [CrossRef] [Google Scholar] [Publisher Link]

[3] G.B. Hmida et al., "Transcutaneous Power and High Data Rate Transmission for Biomedical Implants," *International Conference on Design and Test of Integrated Systems in Nanoscale Technology*, Tunis, Tunisia, pp. 374-378, 2006. [CrossRef] [Google Scholar] [Publisher Link]

[4] Mahammad A. Hannan et al., "Modulation Techniques for Biomedical Implanted Devices and their Challenges," *Sensors*, vol. 12, no. 1, pp. 297-319, 2012. [CrossRef] [Google Scholar] [Publisher Link]

[5] Federal Communications Commission Rules and Regulations, MICS Band Plan, Table of Frequency Allocations, Part 95, 2003.

[6] Kanber Mithat Silay, Catherine Dehollain, and Michel Declercq, "Improvement of Power Efficiency of Inductive Links for Implantable Devices," *2008 Ph.D. Research in Microelectronics and Electronics*, Istanbul, Turkey, pp. 229-232, 2008. [CrossRef] [Google Scholar] [Publisher Link]

[7] F.H. Raab, "Effects of Circuit Variations on the Class E Tuned Power Amplifier," *IEEE Journal of Solid-State Circuits*, vol. 13, no. 2, pp. 239-247, 1978. [CrossRef] [Google Scholar] [Publisher Link]

[8] "C95.1-2005- IEEE Standard for Safety Levels with Respect to Human Exposure to RF Electromagnetic Fields, 3 kHz to 300 GHz," *IEEE Std C95.1-2005 (Revision of IEEE Std C95.1-1991)*, pp.1-238, 2006. [CrossRef] [Publisher Link]

[9] Saad Mutashar Abbas, M.A. Hannan, and A.S. Salina, "Efficient Class-E Design for Inductive Powering Wireless Biotelemetry Applications," *2012 International Conference on Biomedical Engineering (ICoBE)*, Penang, Malaysia, pp. 445-449, 2012. [CrossRef] [Google Scholar] [Publisher Link]

[10] Bert Lenaerts, and Robert Puers, *Omni Directional Inductive Powering for Biomedical Implants*, 1st ed., Springer, 2009. [CrossRef] [Google Scholar] [Publisher Link]

[11] Qingyun Ma et al., "Power-Oscillator Based High Efficiency Inductive Power-Link for Transcutaneous Power Transmission," *2010 53rd IEEE International Midwest Symposium on Circuits and Systems*, Seattle, WA, USA, pp. 537-540, 2010. [CrossRef] [Google Scholar] [Publisher Link]

[12] Koenraad Schuylenbergh, and Robert Puers, *Inductive Powering-Basic Theory and Application to Biomedical Systems*, 1st ed., Springer, 2009. [CrossRef] [Google Scholar] [Publisher Link]

[13] Guillaume Simard, Mohamad Sawan, and Daniel Massicotte, "High-Speed OQPSK and Efficient Power Transfer through Inductive Link for Biomedical Implants," *IEEE Transactions on Biomedical Circuits and Systems*, vol. 4, no. 3, pp. 192-200, 2010. [CrossRef] [Google Scholar] [Publisher Link]

[14] Qingyun Ma, Mohammad Rafiqul Haider, and Yehia Massoud, "A Low-Loss Rectifier Unit for Inductive-Powering of Biomedical Implants," *2011 IEEE/IFIP 19th International Conference on VLSI and System-on-Chip*, Hong Kong, China, pp. 86-89, 2011. [CrossRef] [Google Scholar] [Publisher Link]

[15] Saad Mutashar et al., "Analysis of Transcutaneous Inductive Powering Links," *2012 4th International Conference on Intelligent and Advanced Systems (ICIAS2012)*, Kuala Lumpur, Malaysia, pp. 64-67, 2012. [CrossRef] [Google Scholar] [Publisher Link]

[16] M.A. Adeeb et al., "An Inductive Link-Based Wireless Power Transfer System for Biomedical Applications," *Active and Passive Electronic Components*, vol. 2012, pp. 1-11, 2012. [CrossRef] [Google Scholar] [Publisher Link]

[17] Michael W. Baker, and Rahul Sarpeshkar, "Feedback Analysis and Design of RF Power Links for Low-Power Bionic Systems," *IEEE Transactions on Biomedical Circuits and Systems*, vol. 1, no. 1, pp. 28-38, 2007. [CrossRef] [Google Scholar] [Publisher Link]

[18] Aref Trigui et al., "Maximizing Data Transmission Rate for Implantable Devices over a Single Inductive Link: Methodological Review," *IEEE Reviews in Biomedical Engineering*, vol. 12, pp. 72-87, 2019. [CrossRef] [Google Scholar] [Publisher Link]

[19] Aref Trigui et al., "Inductive Power Transfer System with Self-Calibrated Primary Resonant Frequency," *IEEE Transactions on Power Electronics*, vol. 30, no. 11, pp. 6078-6087, 2015. [CrossRef] [Google Scholar] [Publisher Link]

[20] Alanson P. Sample, David T. Meyer, and Joshua R. Smith, "Analysis, Experimental Results, and Range Adaptation of Magnetically Coupled Resonators for Wireless Power Transfer," *IEEE Transactions on Industrial Electronics*, vol. 58, no. 2, pp. 544-554, 2011. [CrossRef] [Google Scholar] [Publisher Link]

[21] Guoxing Wang et al., "Design and Analysis of an Adaptive Transcutaneous Power Telemetry for Biomedical Implants," *IEEE Transactions on Circuits and Systems I: Regular Papers*, vol. 52, no. 10, pp. 782-787, 2005. [CrossRef] [Google Scholar] [Publisher Link]

[22] Grant Anthony Covic, and John Talbot Boys, "Modern Trends in Inductive Power Transfer for Transportation Applications," *IEEE Journal of Emerging and Selected Topics in Power Electronics*, vol. 1, no. 1, pp. 28-41, 2013. [CrossRef] [Google Scholar] [Publisher Link]

[23] S.Y.R. Hui, Wenxing Zhong, and C.K. Lee, "A Critical Review of Recent Progress in Mid-Range Wireless Power Transfer," *IEEE Transactions on Power Electronics*, vol. 29, no. 9, pp. 4500-4511, 2014. [CrossRef] [Google Scholar] [Publisher Link]

[24] Reem Shadid, Sima Noghanian, and Arash Nejadpak, "A Literature Survey of Wireless Power Transfer," *2016 IEEE International Conference on Electro Information Technology (EIT)*, Grand Forks, ND, USA, pp. 782-787, 2016. [CrossRef] [Google Scholar] [Publisher Link]

[25] Jordi Sacristán-Riquelme, Fredy Segura, and M. Teresa Osés, "Simple and Efficient Inductive Telemetry System with Data and Power Transmission," vol. 39, no. 1, pp. 103-111, 2008. [CrossRef] [Google Scholar] [Publisher Link]

[26] Farzad Asgarian, and Amir M. Sodagar, "Wireless Telemetry for Implantable Biomedical Microsystems," *Biomedical Engineering, Trends in Electronics, Communications and Software*, Intechopen, 2011. [CrossRef] [Google Scholar] [Publisher Link]

[27] Saad Mutashar Abbas et al., "Designing Transcutaneous Inductive Powering Links for Implanted Micro-System Device," *International Journal of Computer and Systems Engineering*, vol. 6, no. 12, pp. 1377-1382, 2012. [Google Scholar] [Publisher Link]